ISJ 22: 30-48, 2025 ISSN 1824-307X

RESEARCH REPORT

Transcriptome analysis of *Apostichopus japonicus* early in the regeneration process after evisceration

BC Wu[1,a], HF Dang[1,3,a], XH Wang, Q Li[2], W Zhou[1], J Liu[1],SG Ye[1],RJ Li[1*]

[a]These authors contributed equally to this work are considered to be the first author together

[1]Agriculture Department Key Laboratory of Mariculture & Stock Enhancement in North China's Sea, Dalian Key Laboratory of Marine Animal Disease Control and Prevention, Dalian Ocean University, Dalian 116023, China [2]China Fisheries College of Tianjin Agricultural University, Tianjin 300384, China [3]Shanghai Aquatic Wildlife Conservation and Research Center, Shanghai, China

 Accepted May 8, 2025

Abstract

In extreme salt stress and anaerobic conditions, *Apostichopus japonicus* survives by "evisceration." The species can eject its viscera and create a new organ if the habitat is suitable. The molecular response of *A. japonicus* coelomocytes and visceral regeneration is examined. Previous research found *A. japonicus* coelomocyte volume recovery 2 h-p-e (two hours post-evisceration) mirrored fast human hematopoiesis. Coelomocytes returned to pre-evisceration levels 6 h-p-e (six hours post-evisceration). First, KCL solution was artificially injected at *A. japonicus* body mass. Subsequently, evisceration occurred. Immunological tissue coelomocytes were taken at 2 h and 6 h-p-e, and those from the control group (0 h) were also collected. Coelomocyte transcriptome was sequenced. Transcriptome sequencing was applied to the collected coelomocytes. At 2 h-p-e, 860 differentially expressed genes were identified, with 639 upregulated and 221 downregulated. At 6 h-p-e, 1638 genes were upregulated and 432 downregulated. Immunity genes were predominantly differentially expressed in the 'Molecular function' category, the major category for these immunity - related differentially expressed genes. Gene differences were analyzed using KEGG annotation. At 2 h-p-e, by comparing the gene expression of *A. japonicus* coelomocytes with that of the non - eviscerated control group (0h), 860 DEGs were identified. These DEGs were associated with 53 pathways, 22 of which were related to illnesses and the immune system, like the ECM - receptor interaction pathway. 6 h-p-e, 20 major enrichment routes were selected, and 11 of them, including the Phagosome pathway, were associated with regeneration. After sequencing data validation, immune genes with substantial alterations were randomly selected for RT-qPCR validation. This experiment revealed that genes related to the ECM-receptor interaction pathway were upregulated at both 2 and 6 h-p-e, which were crucial for early regenerative immunity. Genes in the phagosome pathway were upregulated at different times and play a key role in early immunity. Genes in the lysosome pathway were upregulated at 2 hours and are involved in the immune process. Genes in the Notch signaling pathway were upregulated at 6 hours and may be involved in early vascular regeneration. These findings indicate that coelomocytes and immunological factors have complex and coordinated effects on the immune system of *A. japonicus* after evisceration.

Key Words: *Apostichopus japonicus*; transcriptome; immunization; RT-qPCR

Introduction

In the event of an enemy encounter, *A. japonicus* has a unique defense mechanism known as "evisceration," which allows it to expel internal organs (such as the digestive tract, respiratory tree, and gonads). When the environmental conditions are favorable, new, fully functional organs can rapidly regenerate. (Xue *et al*., 2015). Cell division and cell mortality are two critical processes that regulate the number of cells in multicellular organisms, and evisceration initiates substantial cell proliferation activity. This equilibrium can be adjusted to accommodate specific physiological

Corresponding author:
Ruijun Li
Dalian Ocean University
Heishijiao Street 52, Dalian 116023, China
E-mail: liruijun@dlou.edu.cn

Table 1 Primers used in RT-qPCR

Target gene	Nucleotide sequence of primer (5'-3')
POL4	TACCCGTTGGACAGAGGCTT
	AATACCCCGTGGTTTCCTGC
NEK1	CATTTCAGATGACAGAAGCAGTGG
	CTTTCATCAGCAACACTTGGGTCT
FSIP1	CTCAGGGTAACCAGGATGTAAT
	CTCACAGAGGGAGTGCTACATA
FCN2	TTATCGTGATTGGTCTGAGT
	CTAAAGGATGAATAGAGGGC
NOS1	GGTGTGGAAAAGCCTGGAAC
	CTACCTTTTCCGAGCAGCGT
Novel0428 (A novel gene with significantly expressed levels obtained from transcriptome sequencing)	TTGATGGTTGTCTGCTGCCTC
	TACCTCACTGTGCTTGCCTTG
Lectin	ACTATTTGTGGTCCTGTTTGTGAGC
	TTTTCCTCAGATGAAGTAATGGTGG

processes, including tissue growth and regeneration, despite the strict regulation of the balance between cell division and cell mortality. (Chen *et al*., 2011).

A. japonicus possesses humoral and cellular immunity; however, the absence of specific immune tissues and organs renders the coelomocytes and immune factors in the body cavity fluid crucial to its defense against exogenous pathogens (Li *et al*., 2017). The intruding microorganisms are identified and eliminated by *A. japonicus* when it is attacked by pathogenic bacteria. The damage is repaired through the organism's humoral and cellular immunity. (Liu *et al*., 2012; Chen *et al*., 2018).

In our previous study, we discovered that the volume of coelomocytes in *A. japonicus* returned to its average level at the 2 h-p-e, and the total number of coelomocytes returned to its pre-evisceration state for the first time at the 6 h-p-e. (Li *et al*., 2018) This phenomenon was comparable to the rapid hematopoiesis of human beings (Zhuang *et al*., 2007). For this reason, the present study employed transcriptome sequencing technology to investigate the scientific questions of which genes are crucial in regulating the regeneration process of *A. japonicus* at 2 and 6 h-p-e, as well as the immune mechanism involved in this process.

We conducted RNA-Seq analysis of the early stage of the regeneration process in *A. japonicus* at 2 and 6 h-p-e to ascertain the changes in the expression of immune genes and their immune mechanisms during in *A. japonicus*. The immune tissue coelomocytes from the experimental groups at 2 and 6 h-p-e, as well as those from the non-eviscerated control group (0 h), were subjected to transcriptome sequencing. The sequencing results were spliced to obtain high-quality clean reads, which were compared with the reference genome, functionally annotated, and analyzed in terms of gene expression to explore the overall effects of evisceration on gene expression in *A. japonicus*. We investigated the immune mechanism of *A. japonicus* in the early stages of regeneration after evisceration by analyzing differentially expressed genes and screening immune genes.

Materials and Methods

Experimental animals and sampling

The coelomic fluid containing coelomocytes was carefully extracted from *A. japonicus* using a sterile syringe and immediately transferred into 50 mL RNase-free centrifuge tubes. To prevent RNA degradation, all tools and tubes were pre-treated with RNase inhibitors. The samples were kept on ice throughout the collection process to maintain cell integrity. The coelomocytes were collected in 50 ml RNAase-free centrifuge tubes, centrifuged at 5000 r/min for 10 min at 4 °C to remove coelomic fluid, and the precipitated cells were collected and added to a 1 ml TRIzol. The precipitated cells were pipetted 50 times, transferred to 1.5 ml of RNAase-free centrifuge tube, and immediately stored at -80 °C. For each biological replicate, three biological replicates and six technical replicates were established for the samples collected at 0、2 and 6 hours.

RNA extraction

Sixty *A. japonicus* were acquired from Dalian Baofa Marine Precious Products Farming Company. Following seven days of temporary rearing, they were placed in a shaded area for 20 minutes and then weighed. Individuals with a moist weight of 40±5g were selected for the experiment. The investigation was divided into three groups: two experimental groups (2 and 6 h-p-e) and one control group (no evisceration, 0 hours). These groups contained three individuals each. The experimental group was manually eviscerated by injecting 1 ml of 0.35 mol/L KCL solution, and the evisceration duration was recorded.

Table 2 The statistics of the number of transcriptomic sequences from the coelomocytes of *A. japonicus* at 2 and 6 h-p-e and from those of the control group

Items	Groups		
	2h	6h	Control
Statistics of raw reads			
Total raw reads	166447150	151093168	152098736
Statistics of clean reads			
Total clean reads	162694302	143877890	143975314
Total clean bases(G)	24.41	21.57	21.6
Clean reads ration (%)	97.75	95.22	94.66
Q20 percentage (%)	97.74	96.82	97.02
Q30 percentage (%)	94.66	92.59	92.37
GC percentage (%)	40.19	39.68	39.62
Error rate(%)	0.01	0.017	0.01

Table 3 The statistics of the alignment of clean reads' sequence and reference gene

Items	Groups		
	2h	6h	Control
Total mapped reads	94267412	69726365	92699932
Total mapped (%)	64.05%	67.22%	64.44%
Multiple mapped (%)	5.93%	5.58%	6.8%
Uniquely mapped (%)	58.11%	61.64%	57.64%
To “+” (%)	28.99%	30.65%	28.69%
To "-" (%)	29.12%	30.95%	28.95%

IlluminaHiSeq2500^{TM} sequencing and cDNA library construction

For the samples of the experimental groups at 2 hours and 6 hours post-evisceration, as well as the samples of the control group (no evisceration, 0 hours), follow-up treatment was carried out. Beijing Novozymes Science and Technology Co. Ltd. conducted the extraction, purification, analysis of quality, and construction of the cDNA library, as well as the transcriptome sequencing of mRNA. The Illumina HiSeq2500^{TM} sequencing platform was employed for the sequencing.

Bioinformatics analysis

For each sample in this study, the sequencing data amounted to 5 Gigabases. The transcriptome library obtained from each sample was converted into Raw Data through CASAVA base recognition analysis. Subsequently, the RNA sequences (Clean data) were obtained by sifting low-quality reads and removing splices. These sequences were utilized as the fundamental data for this study. Simultaneously, the reference genome for RNA-seq was the entire genome DNA sequence of *A. japonicus*, as reported by Yang Hong *et al*., 2017. By the RNA-seq protocol (Götz *et al*., 2011), the HISAT2 method (Kim *et al*., 2015) and the HTSeq method (Anders *et al*., 2015) were chosen as the comparative analysis methods for the expression of differentially expressed genes at 2 and 6 h-p-e, respectively, and in the control group (no evisceration, 0 h). The FPKM (Fragments Per Kilobase of transcript per Million fragments mapped) quantification method was also executed.

Table 4 The statistics table of the number of genes in different expression levels

FPKM Interval	A3	A6	A9	B3	B4	B5	C 4	C 5	C 8
0~1	18221 (49.16 %)	17909 (48.32 %)	18115 (48.87 %)	23027 (62.13 %)	16581 (44.74 %)	19140 (51.64 %)	16818 (45.38%)	18939 (51.10%)	19395 (52.33%)
1~3	5096 (13.75 %)	4989 (13.46 %)	4851 (13.09 %)	5321 (14.36 %)	4824 (13.02 %)	5924 (15.98 %)	5137 (13.86%)	5960 (16.08%)	5765 (15.55%)
3~15	8841 (23.85 %)	8984 (24.24 %)	8974 (24.21 %)	5621 (15.17 %)	9318 (25.14 %)	7875 (21.25 %)	8790 (23.72%)	7624 (20.57%)	7523 (20.30%)
15~60	3511 (9.47 %)	3826 (10.32 %)	3772 (10.18 %)	1960 (5.29 %)	4574 (12.34 %)	2813 (7.59 %)	4340 (11.71%)	3045 (8.22%)	2828 (7.63%)
>60	1395 (3.76 %)	1356 (3.66 %)	1352 (3.65 %)	1135 (3.06 %)	1767 (4.77 %)	1312 (3.54 %)	1979 (5.34%)	1496 (4.04%)	1553 (4.19%)
sum	37064 (100 %)	37064 (100 %)	37064 (100 %)	37064 (100 %)	37064 (100 %)	37064 (100 %)	37064 (100 %)	37064 (100 %)	37064 (100 %)

Note: 1. A: 0 hours for control, B: 2 h-p-e, C: 6 h-p-e
2. FPKM: is the most frequently employed method for estimating gene expression levels, and it is defined as the number of Fragments per million Fragments per kilobase length from a specific gene. This method considers the impact of sequencing depth and gene length on the count of Fragments.

The HTSeq method was employed in this study to quantify the expression of differentially expressed genes using FPKM quantification. The expressed genes were compared to the GO (Gene Orthology) database and KEGG (Kyoto Encyclopedia of Genes and Genomes) database using BLAST2GO (Götz *et al*., 2011) and KAAS (KEGG Automatic Annotation Server) (Moriya *et al*., 2007). The quantification results were subsequently analyzed using the DESeq2 method (Götz *et al*., 2011) to obtain the list of differentially expressed genes. The DESeq2 method (Love *et al*., 2014) was employed to analyze the quantitative results of differential expression and generate a list of differentially expressed genes based on the information in the Kyoto Encyclopedia of Genes and Genomes (KEGG) database. Subsequently, the GOSeq method (Young *et al*., 2010) used a hypergeometric distribution to perform functional GO enrichment and KEGG pathway enrichment on the differentially expressed genes. Then, the GOSeq method was used for GO enrichment of differentially expressed genes and KEGG pathway enrichment (Young *et al*., 2010).

PCR validation

Primer 5.0 was employed to generate primers for immunity-related differentially expressed genes to confirm the accuracy of Illumina sequencing data (Table 1). The TRIzol method was employed to extract RNA from three biological replicates of the samples, and Takara's reagent was employed to synthesize cDNA. The MonAmpTMchemoHS PCR Mix (High ROX) reagent from Monad was employed as a template, and cytochrome b was employed as an internal reference. The 7500 Real Time PCR system (Applied Biosystems) was employed for real-time tetrafluorescence quantification. The relative expression was calculated using $2^{-\triangle\triangle Ct}$, with three technical replicates per sample.

Results

Transcriptome Data Quality Assessment

Adapter sequences were trimmed from the raw reads, and low-quality reads were removed, resulting in a total of 21.6 Gb (0h), 24.41 Gb (2h), and 21.57 Gb (6h) of high-quality clean reads. Each sample had a Q20 value greater than 96%, a Q30 value greater than 92%, and a GC content greater than 39%, with a base error rate of less than 0.02% (Table 2). The sequence information fully adhered to the Illumina HiSeq sequencing standard.

Results of Reference Sequence Comparison Analysis

The HISAT software analyzed genomic localization of Clean reads. Table 3 shows key percentages: 2 h-p-e group: Total mapped 64.05%, Multiple mapped 5.93%, Uniquely mapped 58.11%; 6 h-p-e group: Total mapped 67.22%, Multiple mapped 5.58%, Uniquely mapped 61.64%; control group: Total mapped 64.44%, Multiple mapped 6.8%, Uniquely mapped 57.64%.In conclusion, the obtained sequence of the 2 h-p-e group, the 6 h-p-e group, and the 0 h-p-e control group exhibited a genomic localization value of over 64%. Additionally, the percentage of sequenced sequences with multiple mapped sites was less than 10%. Consequently, the sequenced sequences of the present study were both accurate and reliable.

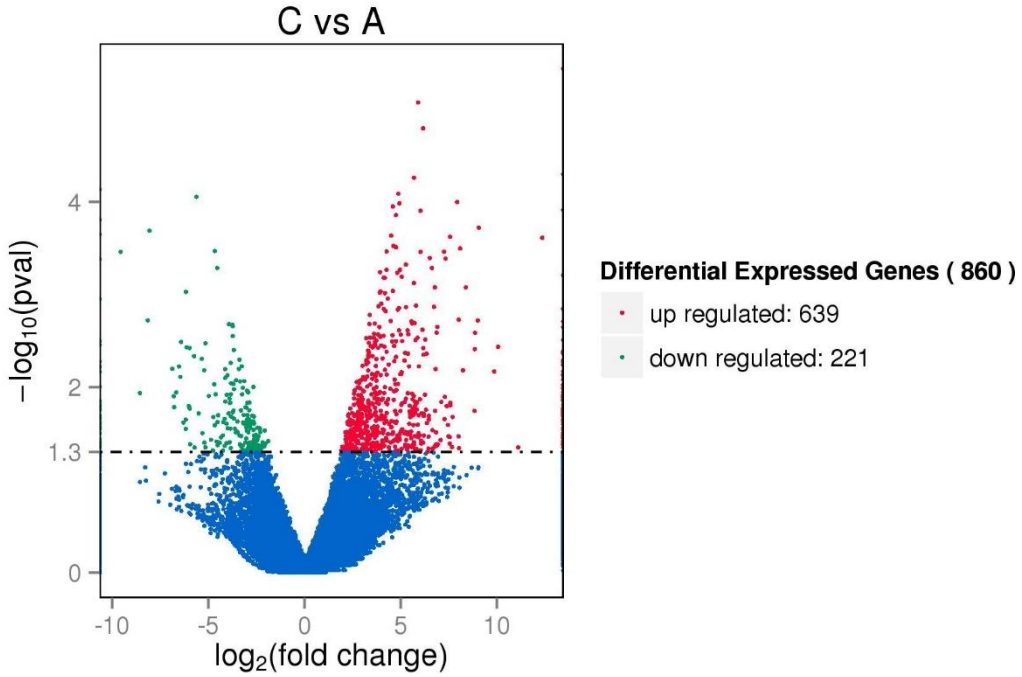

Fig. 1a Volcano plot of *A. japonicus* evisceration 2 h differential genes
Notes:
A: 0 hours for the control group
B: 6 h-p-e
C: 2 h-p-e
Red dots: genes with significant differential expression (up-regulation);
Green dots: genes with significant differential expression (down-regulation);
Blue dots: genes with no significant differential expression;
Horizontal coordinate: gene expression fold change in different samples;
Vertical coordinates: statistical significance of differences in gene expression changes.

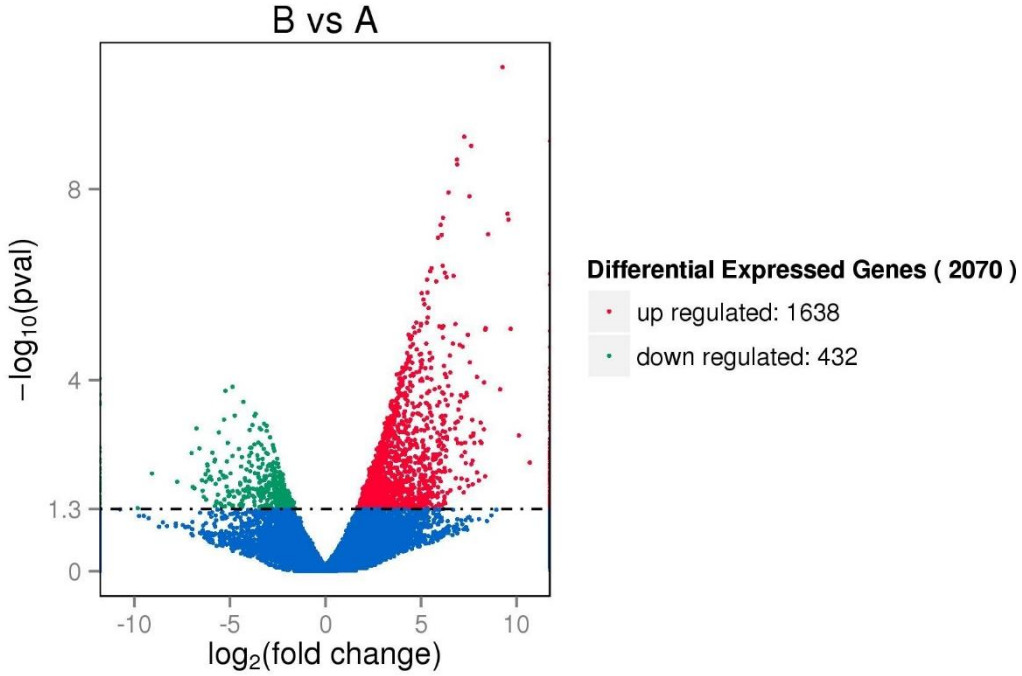

Fig. 1b Volcano plot of *A. japonicus* evisceration 6 h differential genes

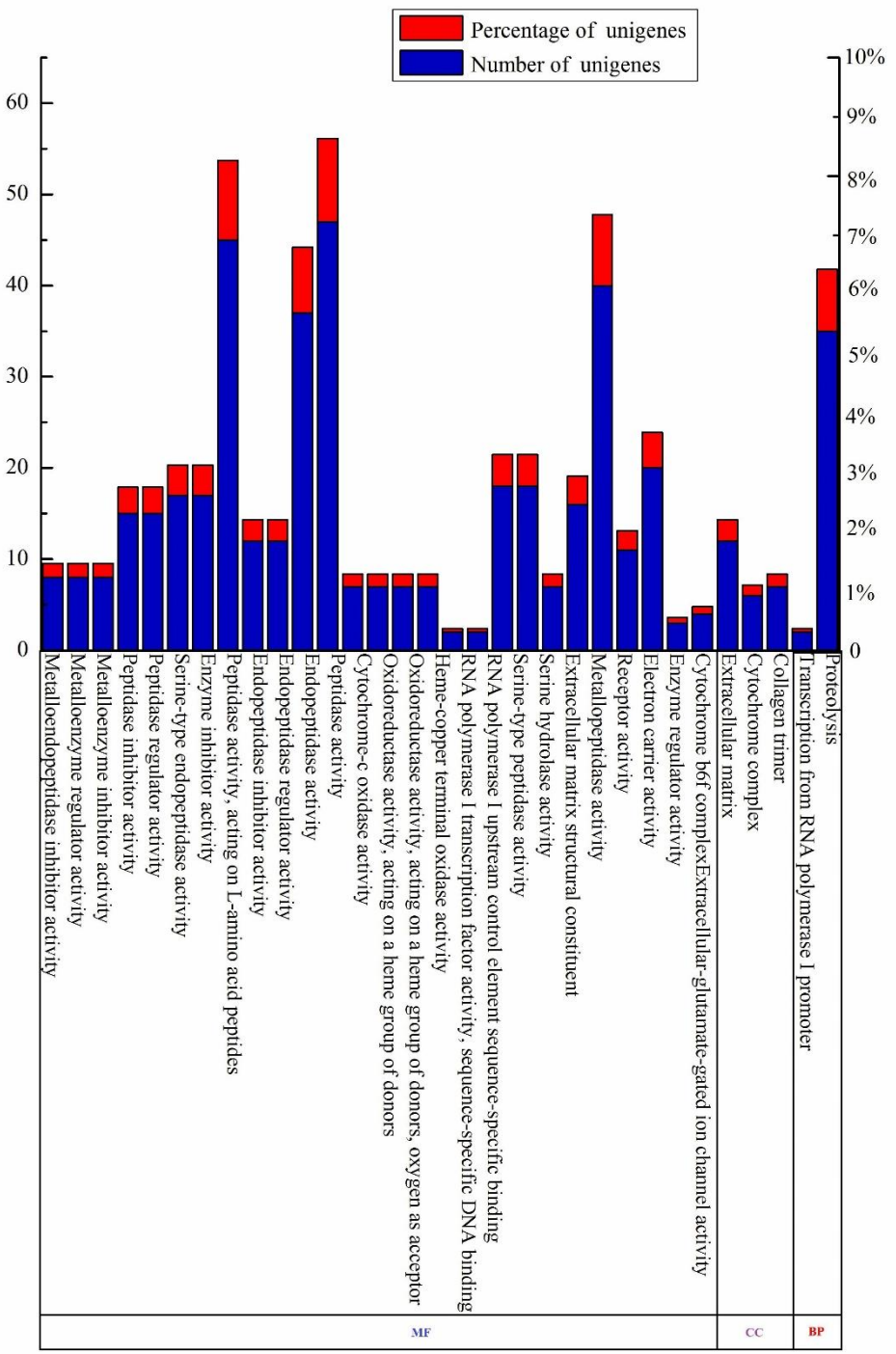

Fig. 2a Gene ontology (GO) analysis of differentially expressed genes in 2 h-p-e
Note: 1. MF: Molecular function; CC: Cellular component; BP: Biological process.
2. Horizontal coordinate: represents the GO term that was enriched.
3. Vertical coordinate: red represents the percentage of differentially expressed genes in the GO term; blue represents the number of differentially expressed genes in the GO term.

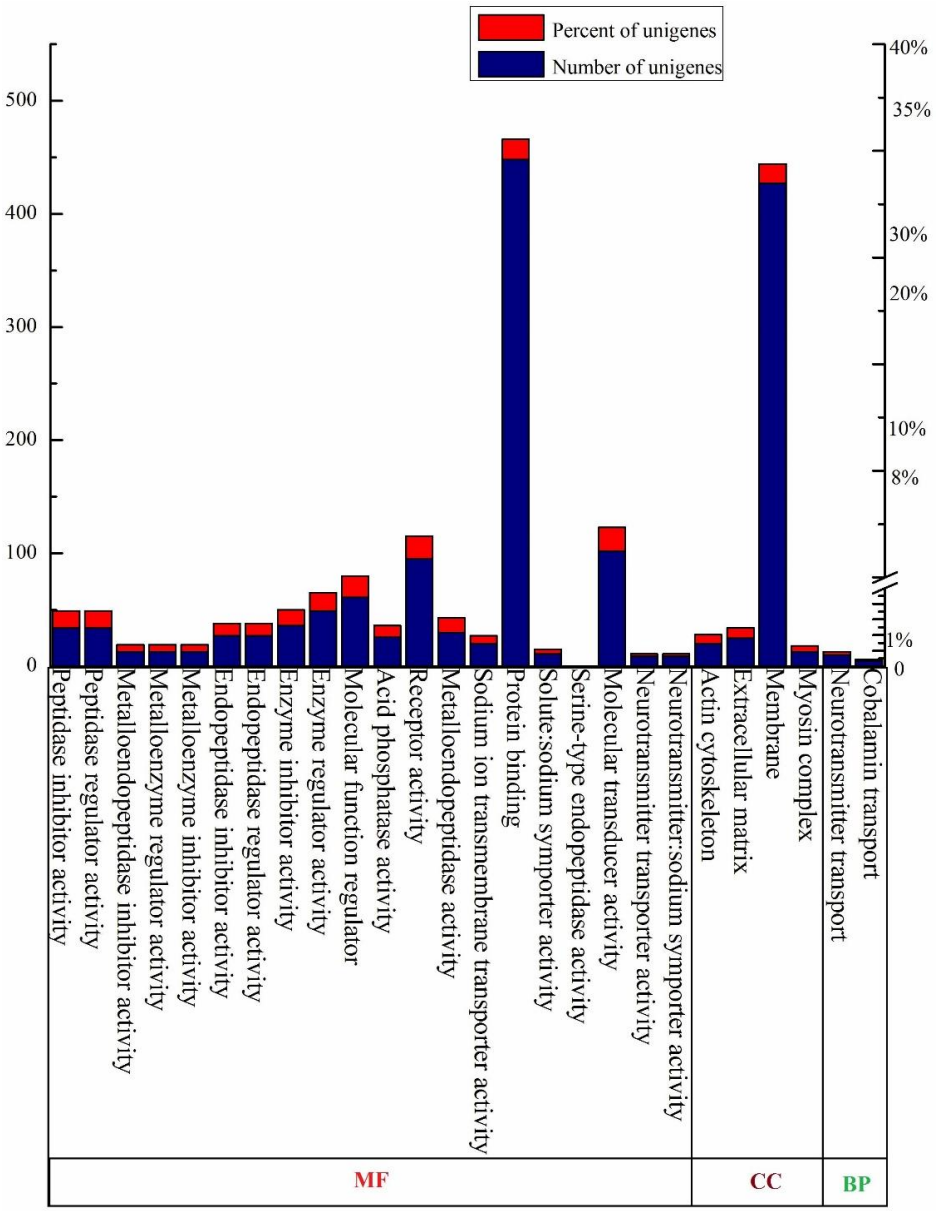

Fig. 2b Gene ontology (GO) analysis of differentially expressed genes in 6 h-p-e
Note: 1. MF: Molecular function; CC: Cellular component; BP: Biological process.
2. Horizontal coordinate: represents the GO term that was enriched.
3. Vertical coordinate: red represents the percentage of differentially expressed genes in the GO term; blue represents the number of differentially expressed genes in the GO term.

Results of gene expression level analysis

The threshold for determining whether a gene was expressed was set at 1, as indicated by the FPKM value. In the experimental group at 2 hours post-evisceration (2 h-p-e), the average number of expressed genes accounted for 47.17% of the total number of genes. In the experimental group at 6 hours post-evisceration (6 h-p-e), this proportion was 50.40%, and in the control group, it was 51.22%. Additionally, in the 2 h-p-e experimental group, the number of genes with an FPKM value less than 1 accounted for 52.83% of the total number of genes in this group. The average proportion of total expressed genes in the 6 h-p-e experimental group was 49.6%, and in the control group, it was 48.78%. (Table 4).

Results of differential expression analysis between the two groups

The gene expression of *A. japonicus* was compared at 0h, 2 h, and 6 h to detect gene expression in the early post-evisceration period. Using DESeq software, expression genes with a significant difference were defined as having a fold

Table 5 Regeneration-related and immune-related expression genes the 2 hours after evisceration coelomocytes of sea cucumber *A. japonicus.* The following table lists the fold change of each immune-related or regeneration-related gene

Gene ID	Gene name	Description	Fold change
ECM-receptor interaction			
BSL78_20648	*COLP3alpha*	3alpha procollagen	4.0634
BSL78_20847	*COLP3alpha*	3alpha procollagen	4.127
BSL78_20650	*COLP1alpha*	Alpha-1 collagen	3.7387
BSL78_00552	*COLP1*(v)	Collagen alpha-1(V) chain	3.2837
BSL78_00551	*COLP1*(v)	Collagen alpha-1(V) chain	2.4801
BSL78_06904	*TSP-A*	Thrombospondin A	2.5862
BSL78_12447	*INTL9*	Integrin alpha-9	2.8558
Lysine degradation			
BSL78_16770	*HLNASH1*	Histone-lysine N-methyltransferase ASH1	-2.3295
BSL78_24277	*HLNH3-79*	Histone-lysine N-methyltransferase, H3 lysine-79	-6.166
BSL78_03903	*HLNMSETD2*	Histone-lysine N-methyltransferase SETD2	2.3058
BSL78_23543	*HLNM*	Histone-lysine N-methyltransferase	-2.4003
BSL78_09673	*HLNM*	Histone-lysine N-methyltransferase	-2.6229
Phagosome			
BSL78_22514	*CDIHC1*	Cytoplasmic dynein 1 heavy chain 1	-2.0879
BSL78_12694	*CATL1*	Cathepsin L1	2.7781
BSL78_12693	*CATL1*	Cathepsin L1	2.3185
BSL78_16663	*CATL1*	Cathepsin L1	2.7197
BSL78_25603	*C3*	Complement component C3	-2.6593
BSL78_06904	*TSP-A*	Thrombospondin A	2.5862
Dorso-ventral axis formation			
BSL78_19762	*PCET2B*	Protein c-ets-2-B	3.5195
BSL78_21511	*PCET2B*	Protein c-ets-2-B	3.7307
BSL78_21510	*PCET2B*	Protein c-ets-2-B	4.5824
Fatty acid biosynthesis			
BSL78_11659	*LCFACSBG2*	Long-chain-fatty-acid--CoA ligase ACSBG2	2.984
BSL78_11660	*LCFACSBG2*	Long-chain-fatty-acid--CoA ligase ACSBG2	5.6199
Lysosome			
BSL78_12694	*CATL1*	Cathepsin L1	2.7781
BSL78_12693	*CATL1*	Cathepsin L1	2.3185
BSL78_16663	*CATL1*	Cathepsin L1	2.7197
Novel05820	*SAPOSIN*	Prosaposin	2.3474
BSL78_11172	*LAMP2*	Lysosome membrane protein 2	2.7929
BSL78_17115	*NPC2*	NPC intracellular cholesterol transporter 2 homolog	4.932
Notch signaling pathway			
BSL78_08346	*DELTA*	Delta protein	2.8178
BSL78_08345	*DELTA*	Delta protein	2.7716
Peroxisome			
BSL78_25196	*CATOACE*	Carnitine O-acetyltransferase	2.4599
Novel02032	*MPV17*	Mpv17-like protein	2.4599
Novel01843	*SERPM*	Serine--pyruvateaminotransferase, mitochondrial	-4.7441
Neuroactive ligand-receptor interaction			
Novel04662	*GAMBRS*	Gamma-aminobutyric acid type B receptor subunit 2	Inf
BSL78_29989	*DRD1L*	D(1)-like dopamine receptor	5.2416
BSL78_08110	*OPRM*	Mu-type opioid receptor	5.6136
mRNA surveillance pathway			
BSL78_28440	*PCF11*	Pre-mRNA cleavage complex 2 protein	-3.2661
BSL78_25168	*PCF11*	Pre-mRNA cleavage complex 2 protein	-3.1637
BSL78_07201	*ERF1*	Eukaryotic peptide chain release factor subunit 1	3.1387
Riboflavin metabolism			
BSL78_06946	PPA5	Tartrate-resistant acid phosphatase type 5	2.8996
Fatty acid degradation			
BSL78_11659	*ACBG2*	Long-chain-fatty-acid--CoA ligase ACSBG2	2.984
BSL78_11660	*ACBG2*	Long-chain-fatty-acid--CoA ligase ACSBG2	5.6199
Glycine, serine and threonine metabolism			
Novel01843	*SERPM*	Serine--pyruvate aminotransferase, mitochondrial	-4.7441
BSL78_07281	*TSAL*	L-threonine ammonia-lyase	3.8249
Glutathione metabolism			
BSL78_05219	*AMPE*	Glutamyl aminopeptidase	2.7151
BSL78_28916	*6 PGD*	6-phosphogluconate dehydrogenase, decarboxylating	2.2034

Table 6 Regeneration-related differential expression following *A. japonicus* after evisceration. Fold changes of regeneration-related gene were listed in the table

Gene ID	Gene name	Description	Fold change
ECM-receptor interaction			
BSL78_20648	*COLP 3alpha*	3 alpha procollagen precursor	5.3538
BSL78_20847	*COLP 3alpha*	3 alpha procollagen precursor	5.0722
BSL78_22684	*ITGBL*	Integrin beta L subunit precursor	2.4814
Novel02680	*ITGBL*	Integrin beta L subunit precursor	2.5866
BSL78_13567	*ITGBL*	Integrin beta L subunit precursor	3.4367
BSL78_06904	*THBS1*	Thrombospondin-1	4.2631
BSL78_09256	*ITGAP*	AlphaP integrin precursor	2.9019
BSL78_18166	*ITGAP*	AlphaP integrin precursor	-2.8734
Phagosome			
BSL78_30137	*ARP1*	Actin related protein 1	4.8908
BSL78_30139	*ARP1*	Actin related protein 1	5.0561
BSL78_27618	*TUBA1*	Tubulin alpha-1 chain	2.7541
BSL78_12379	*TUBBX1*	Tubulin beta chain isoform X 1	2.956
BSL78_12380	*TUBB*	Tubulin beta chain-like	3.458
Novel01876	*LAMP1*	Lysosome-associated membrane glycoprotein 1	1.8514
BSL78_21834	*NOS1*	Nitric oxide synthase, brain isoform X 1	Inf
BSL78_21833	*NOS1*	Nitric oxide synthase, brain isoform X1	6.2537
BSL78_12693	*CATL1*	Cathepsin L 1	3.0398
BSL78_22684	*ITGBL*	Integrin beta L subunit precursor	2.4814
Novel02680	*ITGBL*	Integrin beta L subunit precursor	2.5866
BSL78_13567	*ITGBL*	Integrin beta L subunit precursor	3.4367
BSL78_06904	*THBS1*	Thrombospondin-1	4.2631
TGF-beta signaling pathway			
BSL78_17205	*BMP2/4*	Bone morphogenetic protein BMP2/4 precursor	4.8458
BSL78_03567	*ACVR1X1*	Activin receptor type-1 isoform X 1	2.7298
BSL78_15507	*SMAD5*	Mothers against decapentaplegic homolog 5	2.268
BSL78_15508	*SMAD5*	Mothers against decapentaplegic homolog 5	1.9919
BSL78_06904	*THBS1*	Thrombospondin-1	4.2631
BSL78_01528	*TGFB2*	Transforming growth factor beta-2 proprotein	2.3929
BSL78_07310	*MYC*	Myc protein	2.2059
Notch signaling pathway			
BSL78_08346	*DELTA*	Delta protein	3.6129
BSL78_08345	*DELTA*	Delta protein	3.6006
BSL78_16043	*NCSTN*	Nicastrin	2.3863
Novel03520	*NCSTN*	Nicastrin	2.2241
BSL78_10918	*APH-1*	Gamma-secretase subunit Aph-1-like	3.3761
Peroxisome			
Novel02032	*MPV-17L*	Mpv17-like protein	3.2002
BSL78_26236	*PACOX1X3*	Peroxisomal acyl-coenzyme a oxidase 1 isoform X 3	-2.065
BSL78_06854	*PACOX1X3*	Peroxisomal acyl-coenzyme A oxidase 3	-3.3592
BSL78_18615	*ACSL3*	Long-chain-fatty-acid--CoA ligase 1	-2.346
BSL78_0734	*ACSL3*	Long-chain-fatty-acid--CoA ligase 3	2.1087
BSL78_05022	*ECI2*	Enoyl-CoA delta isomerase 2, mitochondrial	Inf
BSL78_19758	*FAR2*	Low quality protein: fatty acyl-CoA reductase 1	2.8479
BSL78_27853	*PRDX*	Peroxiredoxin	3.926
BSL78_23438	*DHRS4*	Dehydrogenase/reductase SDR family member 4	-2.0679
BSL78_14777	*PEX10*	Peroxisome biogenesis factor 10	-2.6309
BSL78_12748	*CRAT*	Carnitine O-acetyltransferase	-2.6848
Endocytosis			
BSL78_01528	*TGF beta-2*	Transforming growth factor beta-2 proprotein	2.3929
Novel06812	*VEGFR1*	Vascular endothelial growth factor receptor 1	2.8819
BSL78_20400	*HGFR*	Hepatocyte growth factor receptor	2.339
Novel04537	*HGFR*	Hepatocyte growth factor receptor	2.4926
BSL78_20401	*HGFR*	Hepatocyte growth factor receptor	2.5946
BSL78_24105	*CYTH1X1*	Cytohesin-1 isoform X1	1.7555
BSL78_02917	*HSP70PIV*	Heat shock 70 kDa protein IV	2.9001

BSL78_02893	*HSP70PIVL*	Heat shock 70 kDa protein IV-like	3.2604
BSL78_02892	*HSP70PIVL*	Heat shock 70 kDa protein IV-like	2.6286
BSL78_16844	*HSP71*	Heat shock cognate 71 kDa protein	5.0009
BSL78_11973	*HSP71*	Heat shock cognate 71 kDa protein	2.6897
BSL78_16277	*PDCD6IPX2*	Programmed cell death 6-interacting protein isoform X 2	2.1726
BSL78_23140	*RAB22A*	Ras-related protein Rab-22 A	2.7866
Fanconi anemia pathway			
BSL78_17657	*ATRIPX1*	ATR-interacting protein isoform X 1	-2.4166
BSL78_11734	*DNARPREV1L*	DNA repair protein REV1-like	-2.8316
BSL78_11732	*DNARPREV1L*	DNA repair protein REV1-like	-2.8072
BSL78_11733	*DNARPREV1L*	DNA repair protein REV1-like	-1.7657
Novel02613	*DNARPREV1L*	DNA repair protein REV1-like	-2.2515
Novel01378	*LQUNP*	Low quality protein: uncharacterized protein	2.1693
Sphingolipid metabolism			
BSL78_08526	*SPTLC2*	Serine palmitoyltransferase 2	3.1677
BSL78_02074	*SPTLC2*	Serine palmitoyltransferase 2	2.3083
BSL78_03847	*SGPL1*	Sphingosine-1-phosphate lyase 1	3.1733
BSL78_16397	*CERS6X1*	Ceramide synthase 6 isoform X1	2.9032
BSL78_09248	*CERS1*	Ceramide synthase 1	2.9096
BSL78_28082	*CERGLUB*	Ceramide glucosyltransferase-B	2.7217
BSL78_14064	*SIA1*	Sialidase-1	2.4784
BSL78_14008	*ARSA*	Arylsulfatase A	3.3164
BSL78_18602	*PNSMASE*	Putative neutral sphingomyelinase	2.2303
Glycosaminoglycan biosynthesis - heparan sulfate / heparin			
BSL78_07271	*LQEXTL3*	Low quality protein: exostosin-like 3	2.4787
BSL78_07272	*LQEXTL3*	Low quality protein: exostosin-like 3	2.3822
BSL78_08713	*EXT1*	Exostosin-1	3.2817
Nicotinate and nicotinamide metabolism			
BSL78_04999	*PNPX2*	Purine nucleoside phosphorylase isoform X 2	2.1046
BSL78_24145	*PNPX2*	Purine nucleoside phosphorylase isoform X 2	3.4407
BSL78_16088	*CYTN3*	Cytosolic 5'-nucleotidase 3	-4.8616
BSL78_13636	*NICOTINIC*	Nicotinamide/nicotinic acid mononucleotide	2.0335
Jak-STAT signaling pathway			
BSL78_24772	*PROES2B*	Protein enhancer of sevenless 2B isoform X1	2.2872
BSL78_17279	*SOCS2*	Suppressor of cytokine signaling 2	4.4652
BSL78_07310	*MYC*	Myc protein	2.2059

change greater than 2 and a significance level of $P < 0.05$. At 2 hours, 860 differentially expressed genes were identified through screening, with 639 being upregulated and 221 being down-regulated, as illustrated in Figure 1a. At 6 hours, a total of 2070 differentially expressed genes were identified, with 1638 of them upregulated and 432 downregulated, as illustrated in Figure 1b. This method allowed for the inference of the aggregate distribution of differentially expressed genes.

GO enrichment analysis of differentially expressed genes

In order to macroscopically characterize the functional distribution of differentially expressed genes in *A. japonicus* at the early stage of evisceration (2 h, 6 h), functional classification of differentially expressed genes was conducted in consultation with the GO database. The GO enrichment analysis results (Harris *et al*., 2008) indicated that the differentially expressed genes in *A. japonicus* coelomocytes were significantly enriched in three main categories: Molecular function, Cellular component, and Biological processes. The majority of the significant factors were enriched in molecular function and biological processes. The differentially expressed genes were further classified into 32 functional groups in the GO secondary classification at 2 h-p-e and again into 26 functional groups at 6 h-p-e. The differentially expressed genes in each functional group were statistically analyzed, as illustrated in Figure 2.

KEGG enrichment analysis of differentially expressed genes

KEGG enrichment analysis was conducted to extract the differentially expressed genes' pathway annotations and investigate their biological value further. The differentially expressed genes in *A. japonicus* coelomocytes were statistically analyzed for the metabolic pathways that might be implicated by KEGG analysis (Kanehisa *et al*., 2000). We chose the 20 pathway entries with the most significant enrichment at 2 and 6 h-p-e, as illustrated in Tables 5 and 6, to be included in this figure. The ECM-receptor interaction (7 genes, the highest number and highly enriched), Phagosome (6 genes, significantly enriched), and Lysine degradation

pathway (6 genes, significantly enriched) were among the genes that were significantly enriched 2 h-p-e. The ECM-receptor interaction (9 genes, significantly enriched), Phagosome (13 genes, the most numerous and highly significantly enriched), and Notch signaling pathway (5 genes, significantly enriched) were significantly enriched 6 h-p-e (Figure 3). These significantly enriched pathways at different time points are crucial for immunomodulation, signaling, cytokine regulation, and regeneration.

RT-qPCR validation

Researchers randomly carried out RT - qPCR experiments for verification on immune - related differentially expressed genes. Results showed that the fold changes in gene expression detected by RT - qPCR differed from the expression patterns of RNA - Seq, and RNA - Seq showed different sensitivity characteristics in the detection of some genes (as shown in Figure 4).

Discussion

The results of GO enrichment analysis in this study demonstrated that the differential genes of *A. japonicus* coelomocytes were significantly enriched in three categories: cellular component, molecular function, and biological processes. Focusing on the molecular function category, most of the significant factors were enriched here. This indicates that among the differential genes related to immune regeneration post evisceration, those associated with molecular function are prominent. At 6 h-p-e, among the genes enriched for molecular function, protein binding, molecular transducer activity, and endopeptidase activity showed the most significant differential expression. Additionally, receptor activity, molecular function regulator, and enzyme regulator activity were also highly differentially expressed in this category. By comparing these functions within the molecular function category, we can better understand the role of differentially expressed genes in the immune regeneration process post evisceration. For example, protein binding might be crucial for the interaction of various molecules, while molecular transducer activity could be involved in signal transduction pathways, and endopeptidase activity may play a role in protein processing and degradation. It is evident that the molecular transducer activity and receptor activity of differentially expressed genes are crucial at 2 h-p-e and 6 h-p-e.

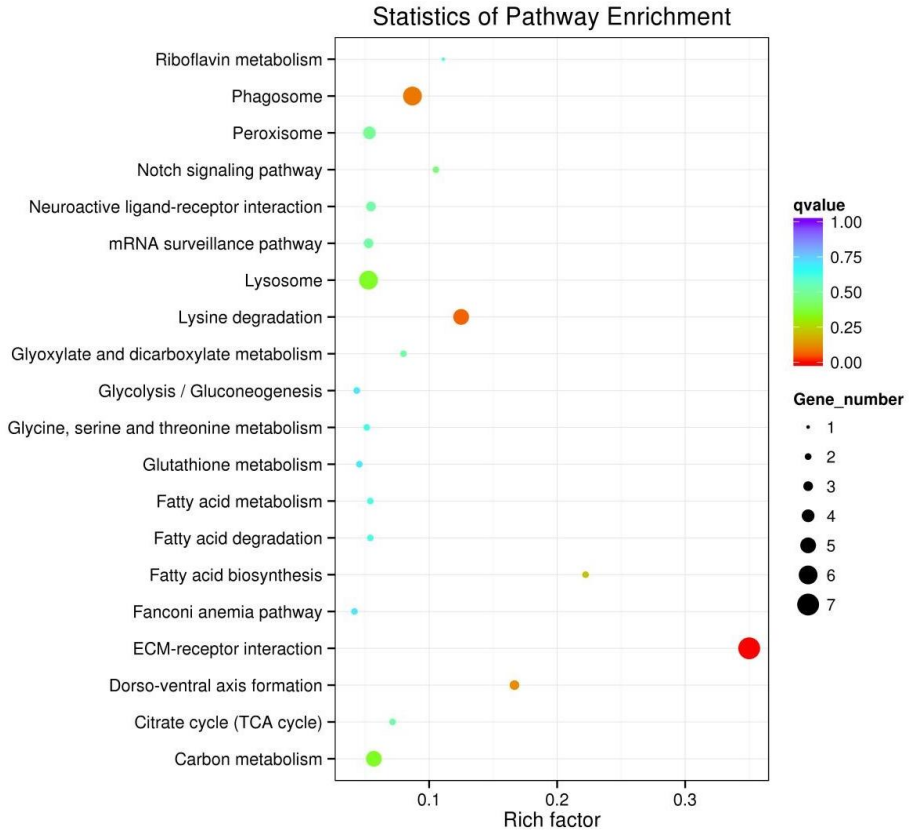

Fig. 3a KEGG analysis of differentially expressed genes 2 h-p-e
Notes:
Vertical axis: pathway name.
Horizontal axis: Rich factor: The more significant the rich factor, the larger the enrichment degree.
Dot size: the number of differentially expressed genes in the pathway.
Color of dots: corresponds to different Q-value ranges from blue to red. Q-value is the P-value after several hypothesis tests and corrections, and the value of Q-value ranges from [0,1]. The closer to zero, the more significant the enrichment.

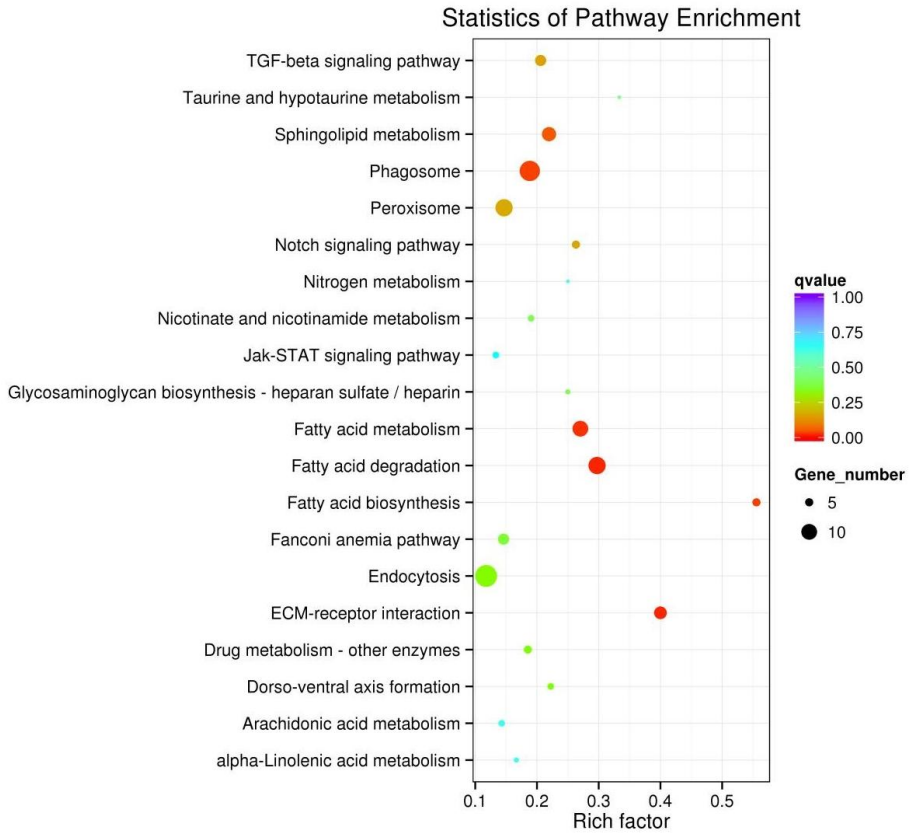

Fig. 3b KEGG analysis of differentially expressed genes 6 h-p-e
Notes:
Vertical axis: pathway name.
Horizontal axis: Rich factor: The more significant the rich factor, the larger the enrichment degree.
Dot size: the number of differentially expressed genes in the pathway.
Color of dots: corresponds to different Q-value ranges from blue to red. Q-value is the P-value after several hypothesis tests and corrections, and the value of Q-value ranges from [0,1]. The closer to zero, the more significant the enrichment.

The differentially enriched genes with the highest number of genes at 6 h-p-e compared to non - eviscerated controls were integrin beta - like 1 (with 6 genes), DNA Repair Protein REV1 - Like (with 4 genes), and hepatocyte growth factor receptor (with 3 genes). These genes were enriched in the Lysosome pathway, the Phagosome pathway, the ECM - receptor interaction pathway, and the Dorso-Ventral Axis Formation pathway, respectively. Furthermore, the differential gene Collagen - Like Protein 3 alpha was enriched in the ECM - receptor interaction pathway at 2 h-p-e and 6 h-p-e. The transcriptome analysis indicated that we screened four pathways in the KEGG pathway that were significantly enriched (Figure 5).

ECM - receptor interaction

We hypothesize that the extracellular matrix - receptor interaction pathway may be a significant factor in the early regeneration immunity after evisceration in *A. japonicus*. The extracellular matrix is reconstructed during the regeneration process, which is a critical biological process (Yannas *et al*., 1989; Kim *et al*., 1997). In multicellular organisms, the extracellular matrix is a critical biological component of the regenerative process. It not only supports and maintains the integrity of cells and tissues but also plays a biological role in guiding the process of cellular genesis and regeneration but also plays a vital role in physiological activities that maintain the structural and functional integrity of the adult body, such as immune response and trauma repair (Zhang *et al*., 2014). Immunity and various diseases are linked to extracellular matrix (ECM) gene abnormalities. Cell - specific interactions with the ECM directly or indirectly regulate cellular activities, including cell adhesion, migration, differentiation, proliferation, and apoptosis (Sun *et al*., 2019). This study identified the regulatory genes in the ECM - receptor interaction pathway associated with the 2 h and 6 h rapid recovery periods following evisceration of *A. japonicus*.

Integrins are critical transmembrane glycoprotein receptors of the ECM - receptor interaction pathway. They facilitate bidirectional signaling between cells and the ECM by binding to

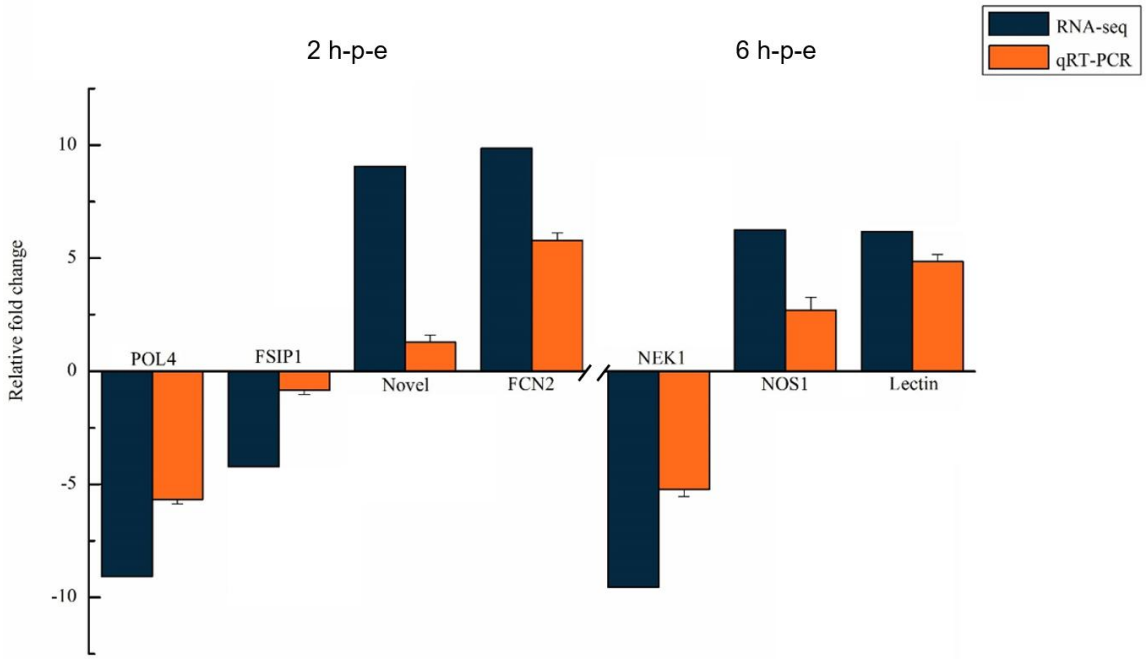

Fig. 4 Verification of the selected DEGs by RT-qPCR as compared with RNA-seq data for 2 h-p-e and 6 h-p-e (two hours post-evisceration and six hours post-evisceration)
Notes:
1. POL4: Retrovirus-related Pol polyprotein from transposon 4
2. FSIP1: Fibrous sheath-interacting protein 1
3. Novel: Transcriptome sequencing yields significantly expressed novel genes
4. FCN2: Ficolin-2
5. NEK1: Serine/threonine-protein kinase Nek1
6. NOS1: Nitric oxide synthase, brain isoform X1
7. Lectin: Lectin genes

ligands and mediating cell - cell and cell - ECM mutual adhesion. (Lin *et al*., 2017) Shingo S, Kaori H, and Nobuchika Y reported in 2018 that integrin α9 subunit blockade exhibits minimal systemic immunomodulatory effects while inhibiting collagen - induced arthritis. (Sugahara *et al*., 2018) Integrin α9 is a component of integrin α9β1, which is essential for the development of lung, lymphatic, and venous valves, wound healing, and cell adhesion and migration. (Wu *et al*., 2012) In the interim, integrin α9β1 is essential for the regulation of cell proliferation and differentiation in various signaling pathways. (Høye *et al*., 2012) Integrin α9β1 interacts with platelet-responsive protein 1 through the presence of numerous ligands. (Mostovich *et al*., 2011) The integrin receptor promotes the development and progression of thyroid cancer in numerous ways after binding to platelet reactive protein and corresponding ligands, including extracellular matrix collagen, intercellular adhesion molecule 1, and vascular cell adhesion molecule. (Wang *et al*., 2013)

Phagosome pathway

We hypothesized that the Phagosome pathway may be crucial in the early immunity of *A. japonicus* during regeneration after evisceration. Phagocytosis is a critical immune system process that is dependent on actin. Initially, immune cells identify exogenous particles and bind to receptors. Subsequently, the cortical cytoskeleton in the cell membrane is reorganized, allowing the particles to be phagocytosed and internalized, resulting in the formation of phagosomes. The phagocytic response in animals is designed to protect against the invasion of pathogenic microorganisms. (May *et al*., 2001) It has been reported that the immune defense function of *A. japonicus* is primarily composed of non-specific immune responses dependent on coelomocyte chemotaxis and phagocytosis. Thus, the cells in the coelom that exhibit phagocytosis have the most direct relationship with the immune defense. (Fang *et al*., 2009; Wang et al., 2009; Ning *et al*., 2014; Yang *et al*., 2014)

In this study, the regulatory genes in the Phagosome pathway involved in the 2 - h and 6 - h rapid recovery periods after evisceration of *A. japonicus* were identified. Actin - related proteins, microtubules, and other related proteins play important roles in various cellular processes. However, their specific functions in *A. japonicus* need further study. (Yao *et al*., 2020) discovered in 2020 that Arp1 - deficient strains may be more susceptible to mortality by ROS - producing immune

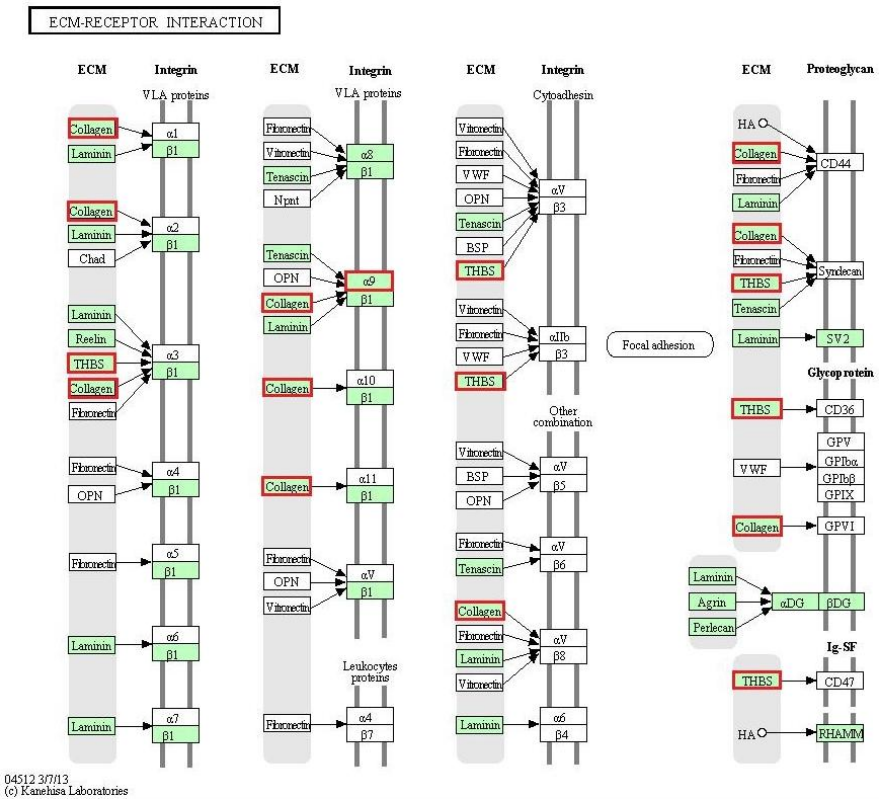

Fig. 5a ECM-receptor interaction pathways generated by KEGG at 2 h-p-e
Note: Images were generated by KEGG; red boxes represent significantly upregulated expressed genes, and blue boxes represent significantly down-regulated genes.

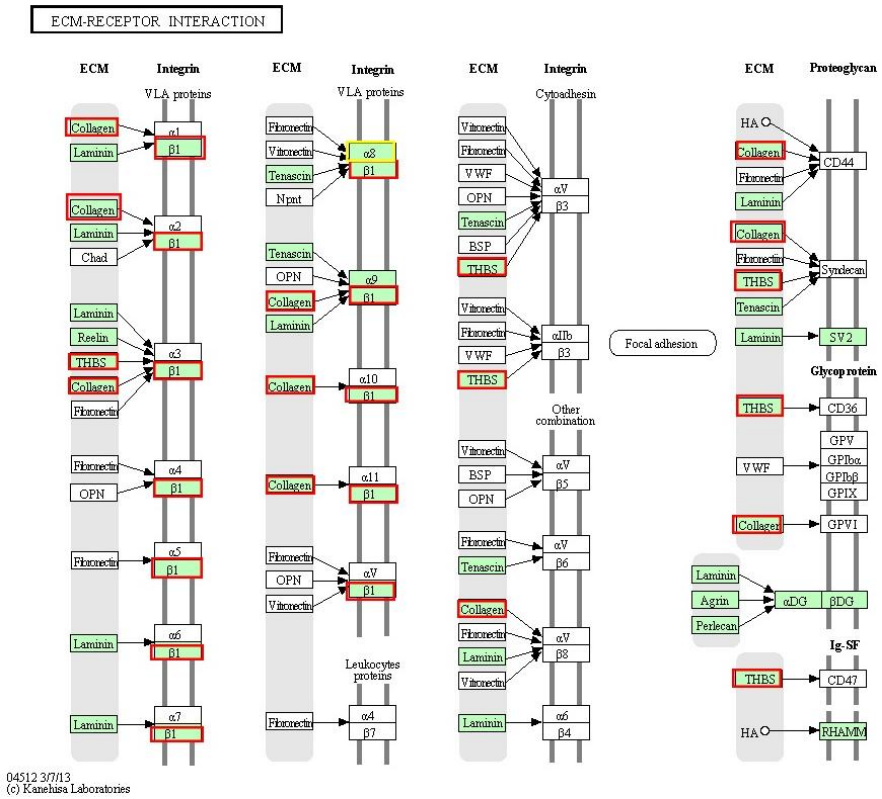

Fig. 5b ECM-receptor interaction pathways generated by KEGG at 6 h-p-e
Note: Images were generated by KEGG; red boxes represent significantly upregulated expressed genes, and blue boxes represent significantly down-regulated genes.

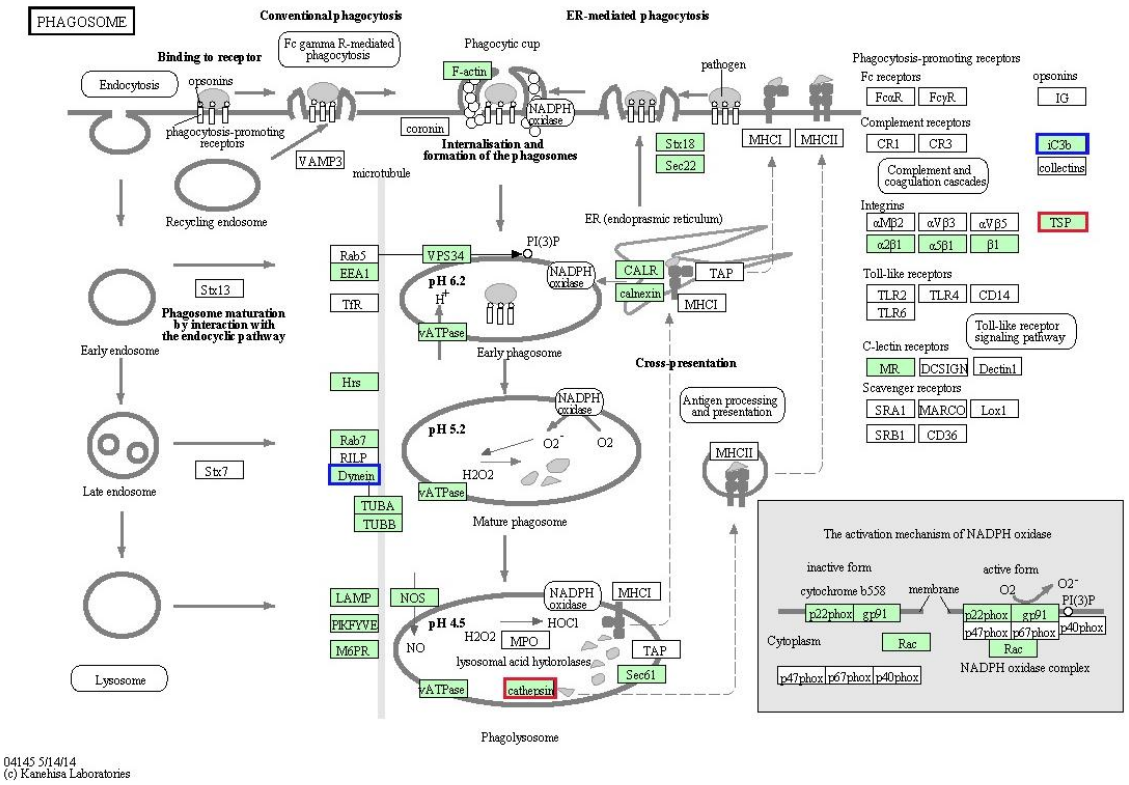

Fig. 6a The Phagosome pathways generated by KEGG at 2 h-p-e
Note: Images were generated by KEGG; red boxes represent significantly upregulated expressed genes, and blue boxes represent significantly down-regulated genes.

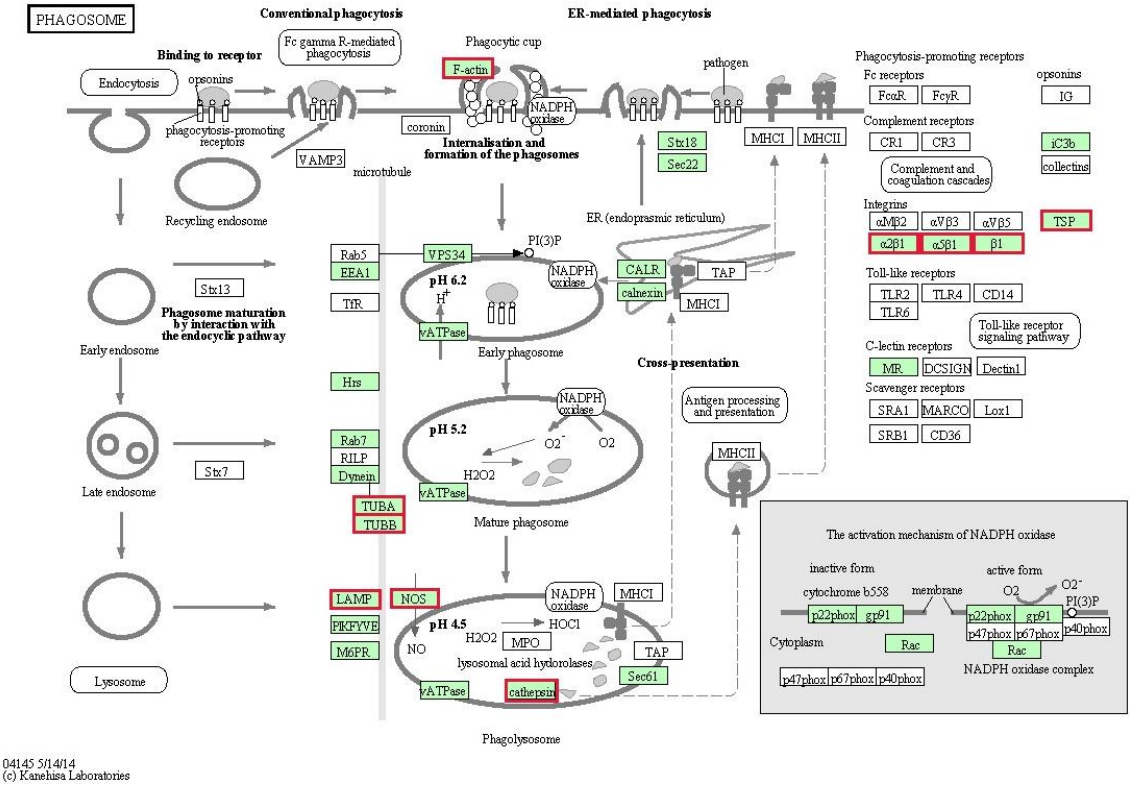

Fig. 6b The Phagosome pathways generated by KEGG at 6 h-p-e
Note: Images were generated by KEGG; red boxes represent significantly upregulated expressed genes, and blue boxes represent significantly down-regulated genes.

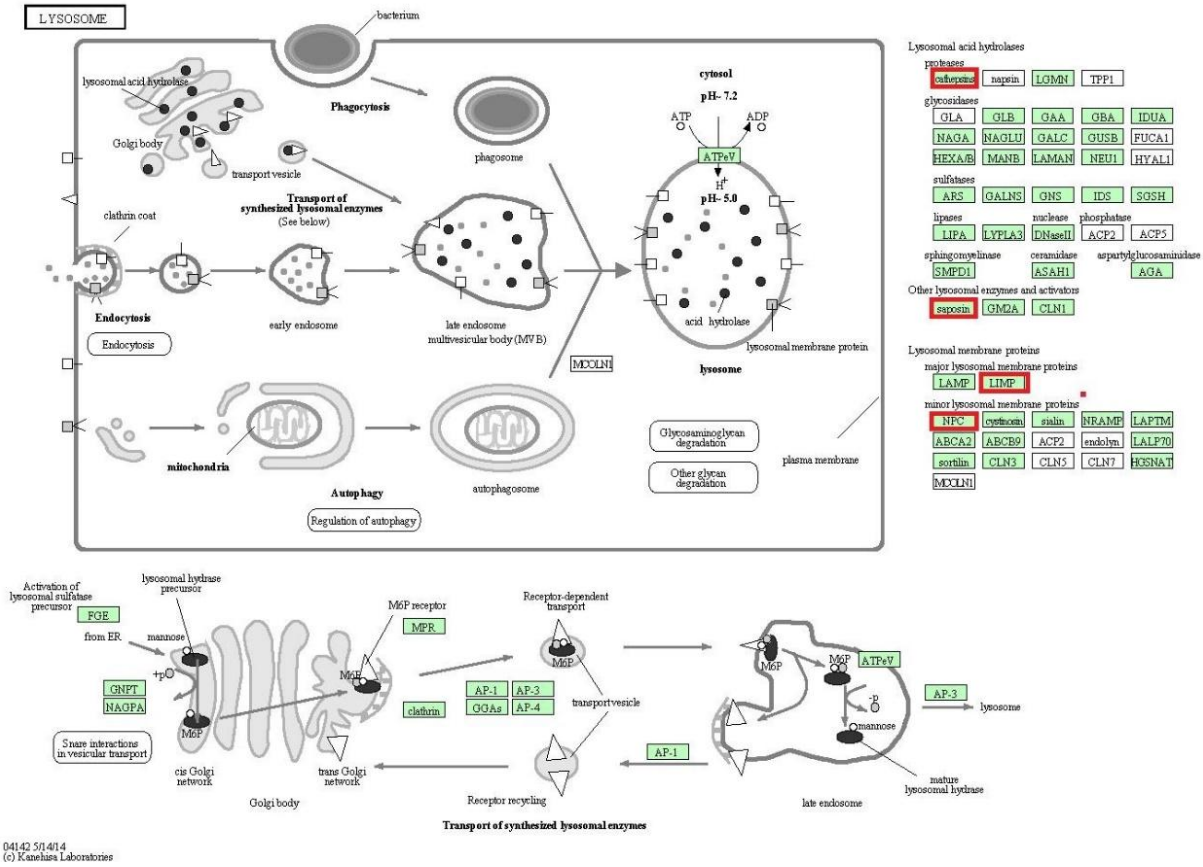

Fig. 7 The Lysosome pathways generated by KEGG
Note: Images were generated by KEGG; red boxes represent significantly upregulated expressed genes, and blue boxes represent significantly down-regulated genes.

cells, such as macrophages and neutrophils. They also suggested that Arp1 is involved in the maintenance of genome stability, which may suggest the existence of potential cell cycle - related morphological regulatory mechanisms. (Yao *et al*., 2020) Microtubules are essential for the maintenance of cell morphology, the facilitation of cell growth and differentiation, and the transportation of materials and signals. (Mitsopoulos *et al*., 2003) Intracellular microtubule proteins are perpetually in a state of depolymerization and assembly. β1 microtubule proteins are crucial for the maturation of megakaryocytes and the induction of thrombopoiesis. The gene THBS1 is involved in platelet polymerization, coagulation, and the regulation of vascular endothelial cell functions. Additionally, it affects tumor progression. (Insalaco L *et al*., 2012; Roka - Moya *et al*., 2014; Kuzmanov A *et al*., 2012; Farberov *et al*., 2014) NOS is the primary rate - limiting enzyme of NO biosynthesis and is involved in many physiological processes. (Shah *et al*., 2004) The relationship between THBS1 and NOS in *A. japonicus* needs further investigation.

Lysosome pathway

We hypothesized that the Lysosome pathway could be instrumental in the immunization of *A. japonicus* by restoring the corpora cavernosa to its normal state during the initial phase of the period following the evisceration of the coelom. The utilization of specific substances, as well as apoptosis, autophagy, and defense. The evisceration process of *A. japonicus* invariably involves the apoptosis of damaged cells. Lysosomes are crucial organelles that are involved in apoptosis and can process a variety of apoptotic signals that are triggered by various external stimuli. (Chen, 2004) Studies have reported that lysosomes are implicated in immunomodulation in *A. japonicus*. (Gao, 2015)

The regulatory genes in the Lysosome pathway that were involved in the 2 - hour rapid recovery period post evisceration in *A. japonicus* were histone L1 (CATL1), lysosomal membrane protein 2 (LYSMP2), sphingolipid (Saposin), and protein NPC2 homolog (PNPC2H). Lysozyme is a defense protein with innate immunity that plays a significant role in the defense of aquatic organisms against bacterial pathogens in the lysosomal pathway. (Wang *et al*., 2011) Lysozyme is a critical component of *A. japonicus*' immune system. (Li, 2016) Saposin is an activating protein that is present in lysosomes and is associated with immune diseases. It is hypothesized that saposin is involved

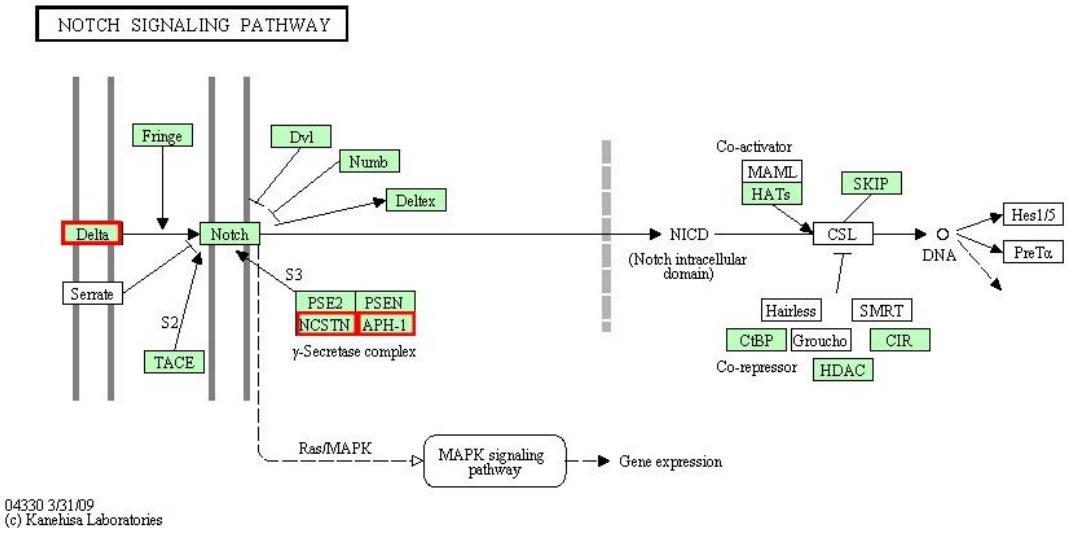

in the early immunity after evisceration of *A. japonicus*. An eosinophilic lysosomal protein hydrolase, protease L, is found in a variety of normal tissue cells and tumor cells in the human body and is significantly expressed in the lysosomal pathway. (Chen, 2004) In 2008, Xu Saitao reported that the proteinase L gene was similar to the one used in the construction and sequence analysis of the sea cucumber cDNA library and the cloning of the histone L gene. (Xu, 2008)

Notch signaling pathway

These findings indicate that the Notch signaling pathway may be involved in the vascular regeneration process of *A. japonicus* during the early evisceration period and may play a critical role in vascular repair. Notch is a group of receptor proteins that are highly conserved and are ubiquitously present on the cell surface. They are responsible for intercellular signaling. The Notch signaling pathway is crucial for the development of vertebrates and invertebrates, as it controls the fate of cells, the formation of organs, and the development of the nervous system. It also plays a critical function in the immune system, particularly tumorigenesis. (Sun L *et al*., 2010)

In this investigation, the regulatory genes in the Notch signaling pathway that were implicated in the 6 - hour rapid recovery period following the evisceration of *A. japonicus* were Delta protein (DELTA), Nicastrin (NCSTN), Gamma - secretase subunit Aph - 1 - like (APH - 1), and *A. japonicus* - like (APH - 1). It has been reported that the Notch signaling pathway plays a significant regulatory role in the regeneration of the biliary perivascular plexus following biliary ischemia - reperfusion injury. (Su, 2015) Delta - like ligand 4 (Dll4) is a critical component of the Notch signaling pathway, which forms blood vessels in both embryonic and adult animals. Additionally, it is involved in the repair of damaged blood vessels and tumor vasculogenesis following ischemia. (Wang *et al*., 2018) Nicastrin and APH - 1 are both components of γ - secretase. The transcription of Notch target genes is initiated by γ - secretase (γ - secretase), which plays a critical role in the activation of Notch signaling following ligand - receptor binding. HERP - 1 and HERP - 3 are smooth muscle - specific effectors in the vascular system, while HERP - 2 acts on the endothelium and smooth muscle layer. The arterial wall is primarily composed of vascular smooth muscle cells, which are responsible for the regulation of arteriogenesis and vascular maturation. (Sun *et al*., 2013) reported that the Notch signaling pathway is substantially expressed in initiating the regeneration of the digestive tract of *A. japonicus* and plays a vital role in the animal's regeneration process. (Zhang *et al*., 2018).

In conclusion, we investigated the mechanisms associated with early immunity during the regeneration process following evisceration in *A. japonicus*. We also summarized the differentially expressed genes and related pathways involved in *A. japonicus*' regenerative immunity. Additionally, similar to *A. japonicus*, the genes and proteins in the coelomocytes of a variety of organisms, including shellfish, are involved in wound repair.

Acknowledgments

This work was funded in part by Liaoning Province "Xingliao Talents" Project (XLYC1808029), and Dalian Key Field Innovation Team Support Program Project (2019RT11).

References

Anders S, Pyl PT, Huber W. HTSeq-a Python framework to work with high-throughput sequencing data. J. Bioinform. 31(2): 166-169, 2015.

Chen L, Chisholm AD. Axon regeneration mechanisms: insights from *C. elegans*. Trends Cell Biol. 21(10): 577-854, 2011.

Chen J, Ren Y, Li Y, Xia B. Regulation of growth, intestinal microbiota, non-specific immune response and disease resistance of sea cucumber *Apostichopus japonicus* (Selenka) in

biofloc systems. Fish Shellfish Immunol. 77: 175-186, 2018.
Cuenca-Zamora EJ, Ferrer-Marín F, Rivera J, Teruel-Montoya R. Tubulin in platelets: when the shape matters. Int J Mol Sci. 20(14): 3484, 2019.
Chen W. Functional characterization of LAPE, a novel apoptosis-inducing protein, from human bone marrow stromal cells: LAPF recruits phosphorylatedp53 (ser-15) to lysosomes-involved apoptotic pathway. Zhejiang University. 2004.
Caiqin W, Wang Huizhen Z. Advances in Notch signaling pathway and vascularization. J. Guangdong Medi. Univ. 6: 687-688, 2010.
Estes J, Baker JV, Brenchley JM, Khoruts A, Barthold JL, Bantle A, *et al*. Collagen Deposition Limits Immune Reconstitution in the Gut. J. Infect Dis. 15;198(4): 456-464, 2008.
Fangyu W, Hongsheng Y, Fei G, Guangbin L. Annual changes of immune enzymes in coelome fluid of sea cucumber, *Apostichopus japonicus*. Institute of Oceanology, Chinese Academy of Sciences. 33(7): 75-80, 2009.
Farberov S, Meidan R. Functions and transcriptional regulation of thrombospondins and their interrelationship with fibroblast growth factor-2 in bovine luteal cells. Biol. Reprod. 91(3): 58, 2014.
Götz S, Arnold R, Sebastián-León P, Martín-Rodríguez S, Tischler P, Jehl MA, *et al*. B2G-FAR, a species-centered GO annotation repository. J. Bioinform. 27(7): 919-924, 2011.
Gundersen GG. Evolutionary conservation of microtubule-capture mechanisms. Nat Rev Cell Biol. 3(4): 296-304, 2002.
Høye AM, Couchman JR, Wewer UM, Fukami K, Yoneda A. The newcomer in the integrin family: Integrin α9 in biology and cancer. Adv. Biol. Regul. 52(2): 326-339, 2012.
Hairong C, Aiqun L, Aiping L, Jianwei Z. Co-localization of JWA proteins with alpha-microtubulin in cells. Chin. Sci. Bull. 3: 229-233, 2004.
He CL, Zhang ML, Wang HY, He JX, Go YX, Li JY. Clinical analysis of THBS1 expression in different gastric mucosal lesions in plateau. Shaanxi Medical Journal. 45(04): 506-507, 2016.
Insalaco L, Gaudio FD, Terrasi M, Amodeo V, Caruso S, Corsini LR, *et al*. Analysis of molecular mechanisms and anti‐tumoural effects of zoledronic acid in breast cancer cells. J. Cell. Mol. Med. 16(9): 2186-2195, 2012.
Jiang J, Zhou Z, Dong Y, Zhao Z, Sun H, Wang B, *et al*. Comparative expression analysis of immune-related factors in the sea cucumber *Apostichopus japonicus*. Fish Shellfish Immunol. 72: 342-347, 2018.
Kim D, Langmead B, Salzberg S L. HISAT: a fast spliced aligner with low memory requirements. J. Nat. Methods. 12(4): 357-360, 2015.
Kanehisa M, Goto S. KEGG: Kyoto Encyclopedia of Genes and Genomes. Nucleic Acids Res. 28(1): 27-30, 2000.
Kim T, Mars WM, Stolz DB, Petersen BE, Michalopoulos, GK. Extracellular matrix remodeling at the early stages of liver regeneration in the rat. J. Hepatol. 26(4): 896-904, 1997.
Kuzmanov A, Wielockx B, Rezaei M, Kettelhake A, Breier G. Overexpression of factor inhibiting HIF-1 enhances vessel maturation and tumor growth via platelet‐derived growth factor‐C. Int J Cancer. 131(5): E603-E613, 2012.
Li C, Ren Y, Jiang S, Zhou S, Zhao J, Wang R, *et al*. Effects of dietary supplementation of four strains of lactic acid bacteria on growth, immune-related response and genes expression of the juvenile sea cucumber *Apostichopus japonicus* Selenka. Fish Shellfish Immunol. 74: 69-75, 2018.
Liu Z, Ma Y, Yang Z, Li M, Liu J, Bao P. Immune responses and disease resistance of the juvenile sea cucumber *Apostichopus japonicus* induced by Metschnikowia sp. C14. Aquac. 368-369: 10-18, 2012.
Li Q, Ren Y, Liang C, Qiao G, Wang Y, Ye S, *et al*. Regeneration of coelomocytes after evisceration in the sea cucumber, *Apostichopus japonicus*. Fish Shellfish Immunol. 76: 266-271, 2018.
Love MI, Huber W, Anders S. Moderated estimation of fold change and dispersion for RNA-seq data with DESeq2. Genome Biol. 15(12): 550, 2014.
Liu W, Sun Y, Cheng Z, Guo Y, Liu P, Wen Y. Crocin exerts anti-inflammatory and anti-arthritic effects on type II collagen-induced arthritis in rats. J. Pharm. Biol. 56(1): 209-216, 2018.
Lin X, Tan S. Advances in integrin alpha 9 and tumors. Chongqing Medical Journal. 24: 129-131+133, 2017.
Li ZS, Lin H. Structure, Function and Related Signaling Pathway of Notch. Chin. J. Cell Biol. 6: 914-921, 2010.
May RC, Machesky LM. Phagocytosis and the actin cytoskeleton. J Cell Sci. 114(6): 1061-1077, 2001.
Moriya Y, Itoh M, Okuda S, Yoshizawa AC, Kanehisa M. KAAS: an automatic genome annotation and pathway reconstruction server. J. Nucleic Acids Res. 35: W182-185, 2007.
Mostovich LA, Prudnikova TY, Kondratov AG, Loginova D, Vavilov PV, Rykova VI, *et al*. Integrin alpha9 (ITGA9) expression and epigenetic silencing in human breast tumors. J. Cell Adh Migr. 5(5): 395-401, 2011.
Meagher RB, Kandasamy MK, Smith AP, McKinney EC. Nuclear actin-related proteins at the core of epigenetic control. Plant Signal Behav. 5:518-522, 2010.
Meagher RB, Kandasamy MK, Smith AP, McKinney EC. Roy, Chapter 5. Nuclear actin-related proteins in epigenetic control. Int Rev Cell Mol Biol. 277: 157-215, 2009.
Mitsopoulos C, Zihni C, Garg R, Ridley AJ, Morris JDH. The prostate-derived sterile 20-like kinase (PSK) regulates microtubule organization and stability. J Biol Chem. 278: 1808-1809, 2003.
Ming L. Effects research of environmental factors and drug residues on the production of ROS by the coelomocytes of *Apostichopus japonicas*. Dalian Ocean University. 2016.

Ning Y, Wenqi W, Lingxu J, Jin Z, Jiankang L. Effects of water temperature on activities of digestive enzymesand immune enzymes in *Apostichopus japonicus*. Marine Sciences. 38(11): 56-59, 2014.

Patel-Hett S, Richardson JL, Schulze H, Drabek K, Isaac NA, Hoffmeister K, *et al*. Visualization of microtubule growth in living platelets reveals a dynamic marginal band with multiple microtubules. Blood. 111(9): 4605-4616, 2008.

Qiong G. Transcriptome Sequencing of CoeIomocyte and Identification and Expression of Immune-related Genes after *Vibrio Splendidus* Infection. Ocean University of China. 2015.

Roka-Moya YM, Zhernossekov DD, Yusova EI, Kapustianenko LG, Grinenko TV. Study of the sites of plasminogen molecule which are responsible for inhibitory effect of Lys-plasminogen on platelet aggregation. Ukr. Biochem. J. 86(5): 82, 2014.

Sun L. Histocvtological events and analysis of key genes during intestine regeneration in Sea cucumber *Apostichopus japonicus* (Selenka). The Institute of Oceanology, Chinese Academy of Sciences. 2013.

Shuli Z, Guangfeng Z, Hongna L, Xiaoyang Q, Yayi H. Proteolipids microsomal Saposin C-dops can enhance immune function in mice. J. Southeast Univ. 27(6): 418-421, 2008.

Srivastava NK, Sharma S, Sharma R, Sinha N, Mandal SK, Sharma D. Metabolic fingerprinting of joint tissue of collagen-induced arthritis (CIA) rat: In vitro, high resolution NMR (nuclear magnetic resonance) spectroscopy based analysis. J. EXCLI J. 17: 257-272, 2018.

Sun HF, Yang X li, Zhao Y, Tian Q, Chen MT, Zhao YY, *et al*. Loss of TMEM126A promotes extracellular matrix remodeling, epithelial-to-mesenchymal transition, and breast cancer metastasis by regulating mitochondrial retrograde signaling. Cancer Lett. 440-441: 189-201, 2019.

Sugahara S, Hanaoka K, Yamamoto N. Integrin, alpha9 subunit blockade suppresses collagen-induced arthritis with minimal systemic immunomodulation. Eur. J. Pharmacol. 833: 320-327, 2018.

Siden-Kiamos I, Schuler H, Liakopoulos D, Louis C. Arp1, an actin-related protein, *Plasmodium berghei*. Mol Biochem Parasitol. 173: 88–96, 2010.

Shah V, Lyford G, Gores G, Farrugia G. Nitric oxide in gastrointestinal health and disease. Gastroenterology. 126(3): 903-913, 2004.

Sha T, Ying Z, Weiwei S, Shiwei Y, Furong L, Li W, *et al*. Effects of anti-LAMP-2 antibody on neutrophil extracellular trap formation. J. Immunol. 11: 968-971, 2012.

Saitao X, Construction and sequence analysis of a sea cucumber cDNA library and cloning of the histone L gene. Dalian Polytechnic University. 2008.

Wang Y, Liu D, Ma Y. Introduction to Immunology. China Traditional Chinese Medicine Publishing House. 91-93, 2013.

Wu J, Zhao M. Effect of integrin α9β1 on corneal neovascularization and vascular endothelial growth factor A expression after corneal suture in rats. J. South. Med. Univ. 32(12): 1704-1707, 2012.

Wang FY, Yang HS, Gao F, Liu, GB. Annual changes of immune enzymes in coelome fluid of sea cucumber, *Apostichopus japonicus*. Marine Science. 33: 75-80, 2009.

Xue Z, Li H, Wang X, Li X, Liu Y, Sun J, *et al*. A review of the immune molecules in the sea cucumber. Fish Shellfish Immunol.. 44(1): 1-11, 2015.

Young MD, Wakefield MJ, Smyth GK, Oshlack A. Gene ontology analysis for RNA-seq: accounting for selection bias. J. Genome Biol. 11(2): R14, 2010.

Yannas IV, Lee E, Orgill DP, Skrabut EM, Murphy GF. Synthesis and characterization of a model extracellular matrix that induces partial regeneration of adult mammalian skin. J. Proc Natl Acad Sci USA. 86(3): 933-937, 1989.

Yang N, Wang WQ, Jiang LX, Zhang J, Liu JK. Effects of water temperature on activities of digestive enzymes and immune enzymes in *Apostichopus japonicas*, Haiyang Kexue (Marine Science), 38(11): 56-59, 2014.

Yao S, Feng Y, Islam A, Shrivastava M, Gu H, Lu Y, *et al*. Loss of Arp1, a putative actin-related protein, triggers filamentous and invasive growth and impairs pathogenicity in *Candida albicans*. Comput. Struct. Biotechnol. J. 4002-4015, 2020.

Yanling W, Dong L, Xiu lW. Advance Of immune-related Genes in Sea cucumber. Biotechnol. Bull. 9: 22-26, 2011.

Zhang X. Hydra extracellular matrix and its function during development and regeneration. Acta Academiae Medicinae Zunyi. 37(1): 6-19, 2014.

Zhang L, Cui M, Ding L, Xia L, Lu J, Shen H. Interleukin-34 aggravates the severity of arthritis in collagen-induced arthritis mice by inducing interleukin-17 production. J. Interferon Cytokine Res. 38(5): 221-225, 2018.

Ziting S. The Role of Notch Signaling Pathway in the Regeneration of Peribiliary Vascular Plexus in ischemia-reperfusion Injury. Kunming Medical University. 2015.

Zhuang W, Su LL, Chen ZQ, Weng MQ, Lin A, Ji Y. Changes of hematological indices of blood donors after 400 ml whole-blood donation, (in Chinese with English abstract). Chin. J. Blood Transfus. 20(4): 287-289, 2007.